Journal of Photochemistry, 5 (1976) 241 - 251

NUMERICAL STUDIES OF THE GROWTH AND DECAY OF RESONANCE FLUORESCENCE: TRAPPING AND QUENCHING OF ARGON 106.7 NM FLUORESCENCE

L. F. PHILLIPS*

Physical Chemistry Laboratory, University of Oxford, Oxford OX1 3QZ (Gt. Britain)

(Received October 1, 1975)

Summary

The growth and decay of the excited atom concentration and of 106.7 nm fluorescence have been calculated, for the case of a cylindrical fluorescence cell having an axial exciting beam, at atom concentrations ranging from 10^{11} to 10^{19} cm^{-3}. The decay of fluorescence is found to occur in two distinct stages, the first corresponding to the spread of excitation from the region of the exciting beam into the body of the fluorescence cell and the second corresponding to the slower escape of excitation from the cell as a whole. Trapping times calculated for the initial fast decay are in good agreement with experimental values in the literature. The effect of variations in the beam diameter, lamp pressure, cell diameter, length of excitation pulse, and quencher concentration have been investigated. In the presence of a quencher Q the trapping times obey a Stern–Volmer equation of the form

$$T_0/T = 1 + k_Q T_0 [Q]$$

where T_0 is the value of the trapping time T in absence of quencher, at T_0/T values up to at least 20. At high quencher concentration the steady-state fluorescence intensity does not decrease as much as the trapping time because Lorentz broadening causes more light to be absorbed from the exciting beam.

Introduction

In a previous communication [1] trapping times were calculated for Cd 228.8 nm and Ar 106.7 nm fluorescence, over a limited range of fluorescer concentrations, in model systems similar to ones which had

* On leave from the University of Canterbury, Christchurch, New Zealand.

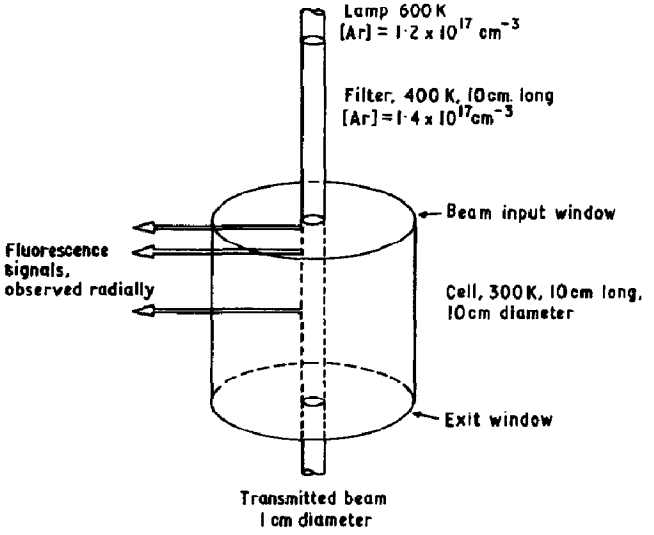

Fig. 1. Model system, with demensions as used in most of the calculations. Fluorescence escapes through the cylinder walls and through both end windows.

been used experimentally [2 - 4]. The trapping time was obtained from the phase-shift between the fundamental components of the fluorescence waveform from the model system and a square-wave excitation pulse. In the present work the trapping time has been obtained from the exponential decay of the fluorescence immediately following the excitation pulse. The lamp + filter + cell configuration that was assumed is shown in Fig. 1, with the dimensions that were used in most of the calculations. Improvements in the computer program allowed the beam diameter to be specified without reference to the number of radial steps in the cell grid, provided for a close spacing of grid steps at the edge of the exciting beam as well as at the edges of the cell, and allowed the grid dimensions to be as large as 14 X 15, 12 X 18, or 10 X 21. For most of the work to be described here a grid with 14 radial steps and 15 axial steps was chosen, in order to obtain maximum information about the radial profiles of the excited atom concentration. Calculated trapping times always differ by less than 5%, and commonly by less than 1%, between corresponding calculations using 10 X 15 and 14 X 15 grids. The program with maximum grid dimensions 10 X 15 occupies 64*k* of core storage; the program which handles the larger grids occupies 115*k* of store.

The equation which is solved is [1]:

$$dU_{KL}/dt = I_{KL} - (Q + T_{KL})U_{KL} + \sum_{MN} (U_{MN} - U_{KL})G_{KLMN} \qquad (1)$$

where U_{KL} is the concentration of excited atoms in the annular volume element specified by the indices K and L, I_{KL} is the rate of absorption of light from the exciting beam in element KL, both at time t, Q is the pseudo-first order quenching rate coefficient, T_{KL} is the rate coefficient for the escape of radiation from element KL to the exterior of the cell,

and G_{KLMN} is the rate coefficient for transfer of radiation from element MN to a point in element KL. The elements of the large matrix G_{KLMN} are given by:

$$G_{KLMN} = G(r_{av}) \cdot R_{KLMN} \cdot \Theta_{KLMN} / 4\pi \tag{2}$$

where Θ_{KLMN} is the average solid angle subtended by element MN from a point on element KL and R_{KLMN} is the average thickness of element MN along a line drawn from the point in element KL. $G(r_{av})$, where r_{av} is an appropriately weighted average distance to element MN from the point in element KL, is obtained by interpolation in a table of $G(y)$ *versus* y, where $G(y)$ is the integral:

$$G(y) = \frac{2A}{k_0 \pi^{1/2}} \int_0^\infty k_\omega^2 \exp(-k_\omega y) d\omega \tag{3}$$

where A is the Einstein coefficient and k_ω is the absorption coefficient at a reduced distance ω from the line centre. An analogous integral $T(y)$, given in eqn. (4), is used in the evaluation of T_{KL} and of the quantities T'_K and T''_K which govern the contribution of element KL to the fluorescence emitted radially:

$$T(y) = \frac{2A}{k_0 \pi^{1/2}} \int_0^\infty k_\omega \exp(-k_\omega y) d\omega \tag{4}$$

In the current version of the program G_{KLMN} is not obtained from eqn. (2), but from the expression:

$$G_{KLMN} = G(r_{av}) V_{MN} / (4\pi r_{av}^2) \tag{5}$$

where V_{MN} is the volume of element MN. This avoids the problems and inaccuracies associated with estimating Θ_{KLMN} and R_{KLMN} individually. The requirement of photon conservation

$$T_{KL} + \sum_{MN} G_{KLMN} \leqslant A \tag{6}$$

has been used to check the accuracy of the G array at small optical depths, where eqn. (6) should tend to an equality. The results indicate that eqn. (5) overestimates G_{KLMN} slightly, on average, presumably because of the manner in which r_{av} is evaluated. The error in the sum of G_{KLMN} over indices M and N is typically a few percent, and amounts to only 15% in the worst case. This degree of error in G_{KLMN} has a negligible effect on calculated trapping times (as was shown by applying appropriate correction factors to the elements of the G_{KLMN} array) because the trapping time is largely governed by the T_{KL} array.

At large optical depths the values of the integrals in eqns. (3) and (4) are controlled by the values of k_ω in the extreme wings of the absorption line. Previously the integrals were evaluated by using Simpson's rule over four ranges of integration, going from 0 to 2.8 in 15 steps of 0.2, from 2.8 to 12.8 in 10 steps of 1.0, and from 12.8 to 62.8 in 10 steps of 5.0. In the fourth range 14 steps of at least 25.0, the actual step size being part

TABLE 1

Effect of the size of the ten ω steps in the extreme wings of the absorption line, beyond $\omega = 62.8$, on calculated trapping times. Sums to infinity use eqns. (7) and (8). [Ar] = 3×10^{16} cm^{-3}. Results at three viewing positions, 0.053, 0.263, and 2.158 cm from the beam input window.

ω step	$T_1(\mu s)$	$T_2(\mu s)$	$T_3(\mu s)$
15	9.66	13.04	17.27
50	9.52	12.81	16.87
150	9.16	12.37	16.14
450	8.43	10.99	13.87
Sums to infinity	9.33	12.64	16.71

of the input data, were used to cover the remainder of the absorption line. However, at large optical depths the calculated trapping times are unduly sensitive to the step size in the fourth range of integration (Table 1). Because the accuracy of the integration suffers when the step size is made very large it is not possible to overcome this effect simply by going to larger and larger step sizes. Therefore the size of the steps in the range beyond $\omega = 62.8$ has been kept below 100 in the most recent calculations and the integration from the maximum value ω_1 to infinity has been performed by summing the series:

$$T_5(y) = a(1 - b/3 + b^2/2.5 - b^3/2.3.7 + b^4/2.3.4.9 - ..) \quad (7)$$

$$G_5(y) = c(1/3 - b/5 + b^2/2.7 - b^3/2.3.9 + ..) \quad (8)$$

where a is $2A\alpha/(\omega_1\pi)$, b is $k_0\alpha y/(\omega_1^2\pi^{1/2})$, and c is $2Ak_0\alpha^2/(\omega_1^3\pi^{3/2})$, and ω_1 is the maximum ω value of the Simpson's rule integrations. The series (7) and (8) result from expanding the exponentials in eqns. (3) and (4) and integrating term by term, using the fact that in the wings of the line k_ω is given by the dispersion formula [5]:

$$k_\omega = k_0\alpha/(\omega^2\pi^{1/2}) \quad (9)$$

The series (7) and (8) converge quite rapidly once the number of terms is greater than the value of b. A series similar to (7) is summed to obtain the contribution from ω_1 to infinity to the rate of absorption from the incident beam, I_{KL}.

Results

Form of the decay curves

Representative decay curves, for 3×10^{14} and 3×10^{16} argon atoms/cm^3, are shown in Figs. 2 and 3, respectively. The curves of both sets are

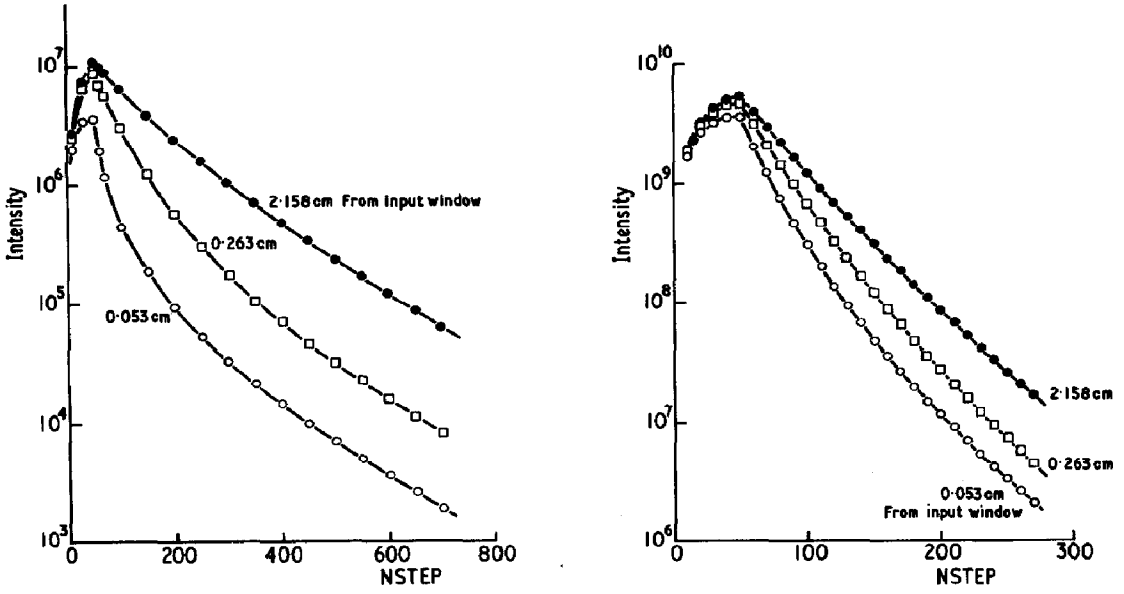

Fig. 2. Decay of fluorescence, at distances from the input window as marked on the curves, [Ar] = 3×10^{14} cm^{-3}, time step duration = 30 ns.

Fig. 3. As in Fig. 2, but for [Ar] = 3×10^{16} cm^{-3}, time step duration = 500 ns.

characterized by an initial rapid decay, followed by a slower decay whose rate is only slightly dependent upon the position of observation. The fast initial transient covers at least an order of magnitude of intensity and its decay time would therefore be expected to be the quantity determined when trapping times were measured by either phase-shift or pulse techniques. This expectation is borne out by the results of the present calculations; the two trapping times generally agree to within 10%.

Excited atom concentration profiles

The concentration profiles in Figs. 4 and 5 are associated with the transient decays at 0.053 cm from the beam input window in Fig. 2 and at 0.263 cm from the input window in Fig. 3, respectively. The curves in Fig. 5 do not correspond precisely to those in Fig. 3, in that the exciting beam in Fig. 5 was turned off at time step 200, instead of at time step 50, so that the decay could be observed from the steady state. The steady state profile is similar to those given previously [1]. Both sets of profiles demonstrate that the fast transient corresponds to the spreading out of the excitation from the beam region into the body of the cell, a process which is superimposed upon the slower escape of radiation from the cell as a whole. The profile at time step 200 in Fig. 5 is only slightly different from that at step 50, so that the slope of the initial transient is not very different for decay from the steady state and for decay after a brief excitation pulse. The dependence of the initial decay rate on the duration of the exciting pulse is given in detail in Table 2 for an argon concentration of 3×10^{16}

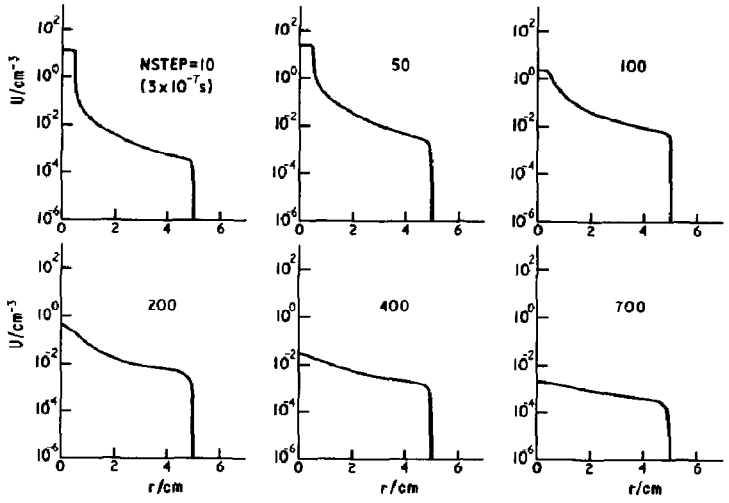

Fig. 4. Radial concentration profiles, 0.053 cm from input window, after the numbers of time steps that are marked on the curves. [Ar] = 3×10^{14} cm^{-3}, time step = 30 ns.

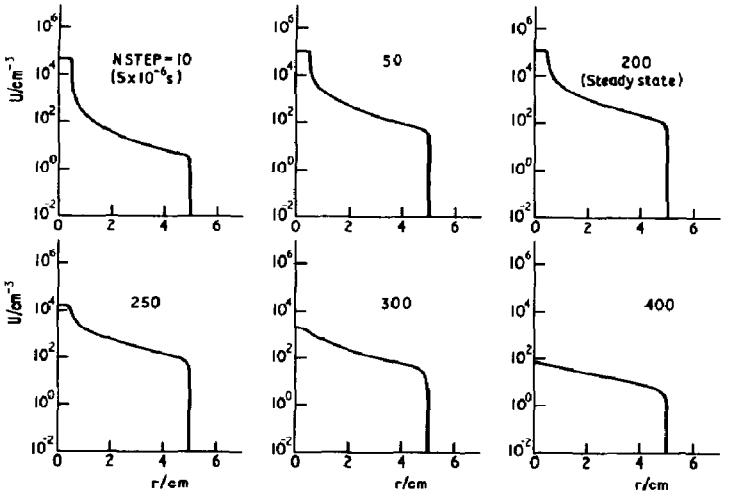

Fig. 5. Radial concentration profiles, 0.263 cm from input window, after the numbers of time steps marked on the curves. [Ar] = 3×10^{16} cm^{-3}, time step = 500 ns.

$atom/cm^{-3}$. The output waveform for the case where the steady state fluorescence intensity is reached is not perfectly symmetrical, in that whereas the initial part of the decay curve can be superimposed exactly, after inversion, upon the initial part of the growth curve, the final decay occurs appreciably more slowly than the last part of the growth to the steady state. The initial decay rate is more dependent upon the diameter of the exciting beam than upon the diameter of the cell, as is demonstrated by the data in Fig. 6. Once again this emphasizes that the initial transient results mainly from the spreading out of the excitation from the region of the exciting beam.

TABLE 2

Effect of exciting pulse duration on the decay rate of the initial transient. Results for 3×10^{16} Ar atoms/cm^3, at 0.053, 0.263 and 2.158 cm from the point of entry of the exciting beam. Trapping time T = 1/decay rate. (ω steps = 100 in wings of line).

t(pulse)(μs)	T(μs) at distances from input window		
	0.053 cm	0.263 cm	2.158 cm
100	9.46	12.67	16.67
30	9.02	12.24	15.94
10	8.57	12.00	15.58
3	8.53	11.98	15.53
1	8.45	11.95	15.48

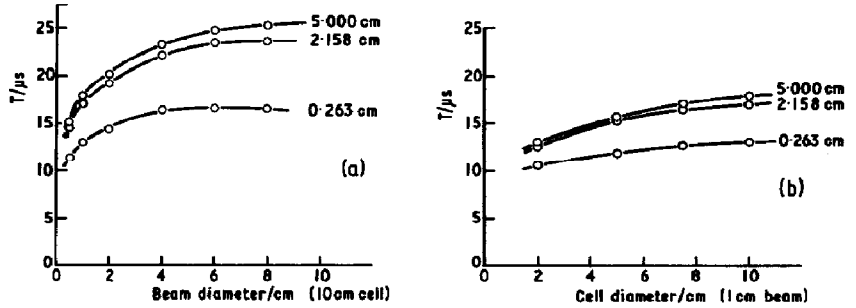

Fig. 6. (a) Variation of trapping time with beam diameter in a 10 cm diameter cell. [Ar] = 3×10^{16} cm^{-3}. Distances from the beam input window as marked on the curves. (b) Variation of trapping time with cell diameter for a 1 cm diameter beam. [Ar] = 3×10^{16} cm^{-3}. Distances from the beam input window as marked on curves. (ω steps = 50 in wings of line; cf. Table 1).

Variation of trapping time with argon pressure

Results are given in Fig. 7 for three distances from the input window for the initial transient decay from the steady state. The limiting value at low pressures is equal to the natural lifetime of 8.3 ns [6]. At high pressures there is good agreement with the experimental data of Wayne and coworkers [3]. At intermediate pressures there is a considerable range over which the trapping time is proportional to the argon pressure. The disagreement with the experimental data at the lowest pressures at which measurements were made can be attributed at least partly to differences between the experimental system and the model, such as the use of a relatively large-aperture "channeltron" detector for the radiation. Differences in the lamp operating pressure, which in the model system acts via the number of absorbing atoms in the filter layer, would affect the observed trapping times by altering the distribution of excited atoms along the beam axis. The

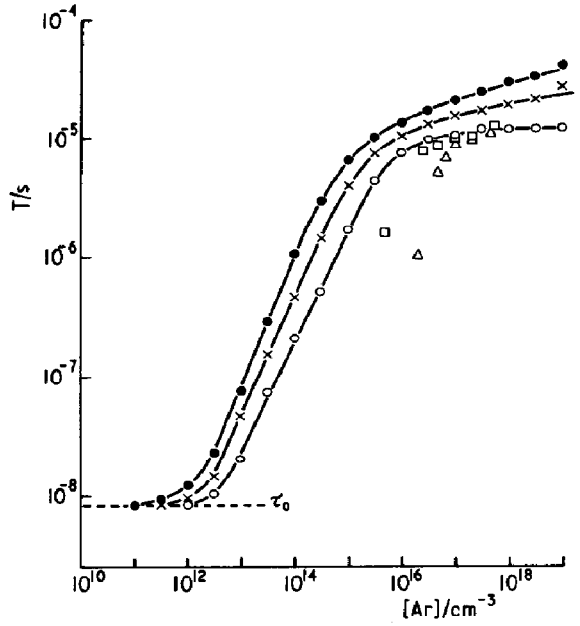

Fig. 7. Variation of trapping time with argon pressure, calculated from initial transient decays from the steady state, distances from the input window (top to bottom), 2.158, 0.263 and 0.053 cm. The squares and triangles are two sets of experimental values from Fig. 8 of ref. 3. Integrations in the wings of the absorption line based on eqns. (7) and (8).

TABLE 3

Variation of calculated trapping time with the argon pressure in the filter layer. Results for three viewing positions as in Table 2. ω step size = 150 in the line wings. [Filter pressure normally used: 1.4×10^{17} cm^{-3}.]

Filter pressure (10 cm path)	T_1(μs)	T_2(μs)	T_3(μs)
[Ar] = 4.2×10^{17} cm^{-3}	9.17	12.39	16.15
1.4×10^{17}	9.16	12.37	16.14
4.2×10^{16}	9.06	12.23	16.10
1.4×10^{16}	8.74	11.95	16.12
4.2×10^{15}	8.36	11.61	16.64
1.4×10^{15}	8.21	11.48	17.85

results given in Table 3 indicate that the effects of variations in lamp pressure should not be very great, at least when the optical depth of the filter layer is large. Related to the effect of varying the lamp pressure is the effect of varying the temperature difference between lamp and fluorescence cell. As the results in Table 4 show, this is also a very small effect when the optical depth of the filter layer is large.

TABLE 4

Effect of varying the temperature of the fluorescence cell. T(lamp) = 600K, T(filter) = 400K, [Ar] = 3×10^{16} cm^{-3} in the cell, 1.4×10^{17} in the filter layer. (Sums to infinity used in line wings; cf. Table 1.)

T(K)	T_1(μs)	T_2(μs)	T_3(μs)
400	9.44	12.63	16.66
300	9.33	12.64	16.60
200	9.36	12.77	16.71

Effect of quenching on the initial transient decay

Rate constants for quenching reactions of Ar($^3P_1$) have previously been determined [4] from decay rates for the initial transient and from steady-state fluorescence intensities, on the basis of the assumption that both the trapping time T and the intensity I obey the Stern–Volmer equation:

$$I_0/I = T_0/T = 1 + k_Q T_0 [Q] \tag{10}$$

where T_0 is the trapping time measured in absence of quencher and k_Q [Q] is identical with the quantity Q which appears in eqn. (1). However, as the authors point out, there is no *a priori* reason to assume that this assumption is even approximately valid, and in fact detailed theoretical considerations [7] suggest that in general it is not likely to be. In part, their work amounts to an experimental test of this assumption, which is shown to be correct within an uncertainty of about ± 15%. Table 5 contains the results of computer simulations for quenching by NO. The Lorentz broadening cross-section was taken as 7×10^{-15} cm^2, and the rate constant k_Q was given its experimental value of 2.6×10^{-10} cm^3 molecule^{-1} s^{-1} [4]. It can be seen that the trapping times T for the model system agree with those predicted from eqn. (10) to within 2%, which lends confidence to the experimentally measured quenching constants. The steady-state intensities do not agree so well with the predicted values, the intensity always being somewhat greater than expected. The discrepancy amounts to 10% at the highest pressure of NO. A similar effect was observed experimentally in the quenching of Hg 253.7 nm fluorescence [8], where it was attributed to the effect of pressure broadening on the rate of absorption of light from the exciting beam. It should be noted that the largest broadening effect in Table 5 is found for an NO pressure of only 0.3 Torr; with a weaker quencher the effect would be relatively more significant.

TABLE 5

Comparison of calculated trapping times and steady state intensities with values predicted from T_0, I_0, k_Q and [Q] = [NO], using eqn. (10). Results for three viewing positions. [Ar] = 10^{16} cm^{-3}, k_Q = 2.6 × 10^{-10} cm^3 molecule^{-1} s^{-1}. ω step size = 250 in line wings.

[NO]	Calculated T (μs)			Predicted T (μs)		
zero	7.009	8.694	10.57			
3 × 10^{14}	4.455	5.146	5.752	4.532	5.181	5.793
1 × 10^{15}	2.444	2.651	2.803	2.483	2.667	2.820
3 × 10^{15}	1.073	1.113	1.139	1.084	1.117	1.143
6 × 10^{15}	0.5835	0.5952	0.6026	0.5873	0.5970	0.6044
1 × 10^{16}	0.3628	0.3674	0.3703	0.3646	0.3683	0.3711
[NO]	Calculated I (× 10^{10} photon/s)			Predicted I		
zero	12.506	15.531	16.868			
3 × 10^{14}	8.056	9.229	9.219	8.086	9.255	9.245
1 × 10^{15}	4.458	4.779	4.516	4.431	4.764	4.501
3 × 10^{15}	1.993	2.040	1.865	1.934	1.996	1.825
6 × 10^{15}	1.110	1.118	1.009	1.048	1.067	0.964
1 × 10^{16}	0.712	0.711	0.638	0.650	0.658	0.592

Conclusions

The problem of radiation trapping could, in a sense, be regarded as solved once Holstein [9, 10] had pointed out the inadequacy of theories based on diffusion of radiation with a finite mean-free-path [11 - 13] and had used the Ritz variation method to solve the Biberman–Holstein equation, of which eqn. (1) is one form. Subsequent work by Walsh [14], Van Trigt [15], and Van Volkenburgh and Carrington [7] extended his solutions in various ways, but the results which were obtained for idealised systems, such as infinite slabs and cylinders with uniform illumination, were not very easy to apply to practical situations. The advantage of the present calculations is that they employ a model which is easy to realize experimentally and is a close approximation to many experimental systems that have been used in the past. The calculation can take account of such experimental variables as beam diameter, cell size, temperature, observation point, extent of reversal of the source line, buffer gas composition, and type of line broadening which is present. The two-layer lamp + filter model which is used for the light source, derived ultimately from the work of Braun and coworkers [16, 17], is also a realistic approximation to a commonly-used type of experimental system. The excellent agreement that has been obtained between experimental and calculated trapping times indicates that the computer program is likely to be of practical value in the future as a predictive tool. Atomic transitions which are of interest for

future work include Lyman-α, the oxygen triplet at 130.5 nm, the nitrogen triplet at 120 nm, and the mercury lines at 184.9 and 235. 7 nm. For the 253.7 nm line it will be interesting to follow Walsh and Holstein and compare the calculated results with the experimental data of Alpert *et al.* [18].

Acknowledgements

The author is grateful to the Oxford University Computer Laboratory for the generous provision of facilities and advice, to Dr R. P. Wayne for helpful discussions and to Professor J. S. Rowlinson for the hospitality of his department.

References

1 L. F. Phillips, J. Photochem., 4 (1975) 407.
2 P. D. Morten, C. G. Freemen, R. F. C. Claridge and L. F. Phillips, J. Photochem., 3 (1974) 285.
3 M. J. Boxall, C. J. Chapman and R. P. Wayne, J. Photochem., 4 (1975) 281.
4 M. J. Boxall, C. J. Chapman and R. P. Wayne, J. Photochem., 4 (1975) 435.
5 A. C. G. Mitchell and M. W. Zemansky, Resonance Radiation and Excited Atoms, Cambridge University Press, London, 1934.
6 W. L. Weise, M. W. Smith and B. M. Miles, Atomic Transition Probabilities I, NSRDS-NBS-4 (1966).
7 G. Van Volkenburgh and T. Carrington, J. Quant. Spectros. Radiat. Transfer, 11 (1971) 1181.
8 R. H. Newman, G. C. Freeman, J. M. McEwan, R. F. C. Claridge and L. F. Phillips, Trans. Faraday Soc., 66 (1970) 2827.
9 T. Holstein, Phys. Rev., 72 (1947) 1212.
10 T. Holstein, Phys. Rev., 83 (1951) 1159.
11 K. T. Compton, Phys. Rev., 20 (1922) 283.
12 K. T. Compton, Phil. Mag., 45 (1923) 752.
13 E. A. Milne, J. London Math. Soc., 1 (1926) 1.
14 P. J. Walsh, Phys. Rev., 116 (1959) 511.
15 C. Van Trigt, Phys. Rev., 181 (1969) 97.
16 W. Braun and T. Carrington, J. Quant. Spectros. Radiat. Transfer, 9 (1969) 1133.
17 W. Braun, A. M. Bass and D. D. Davis, J. Opt. Soc. Am. 60 (1970) 166.
18 J. Alpert, A. O. McCoubrey and T. Holstein, Phys. Rev., 76 (1949) 1257.